Fabrication of Buried Corrugated Waveguides by Wafer Direct Bonding

S. Pélissier, G. Pandraud, A. Mure-Ravaud, A. V. Tishchenko, and B. Biasse

***Abstract*—A new fabrication method of deeply buried corrugated waveguides is presented. It uses a direct bonding process and allows us to make efficient grating couplers in waveguides. The efficiency of the grating is enhanced by enclosing air in its grooves during the fabrication process. A demonstrator based on a waveguide produced by ion exchange has been fabricated and tested. Theoretical and experimental results are compared.**

***Index Terms*—Buried gratings, buried waveguides, coupling gratings, ion exchange, wafer direct bonding.**

I. Introduction

PERIODIC structures in waveguides have many applications [1] such as input or output couplers, mode or polarization converters and filters, wavelength filters or multi-/demultiplexers,... Buried gratings are interesting for different reasons. First of all, it is simply of great interest to bury the corrugated waveguide beneath the surface to avoid pollution and deterioration. Furthermore, it will be shown here that a buried grating has a higher coupling efficiency than a non covered one. When considering gratings as input or output couplers the length of the grating must not be more than a few millimeters to be compatible with photolithography technology and with practical beam dimensions. The optimal coupling length of a grating depends on the size of the beam and on the coupling efficiency [2]. This efficiency is dependent on the value of the field at the grating interface, the index difference, the groove depth and the grating period.

Wafer direct bonding (WDB) is a well known way to join wafers in a stable configuration without adding any adhesive product. It is often used in microsystems technologies [3]. Van der Waals forces are used to adhere to each other well polished and clean wafers. It may be applied to all kind of materials combination but silicon/silicon bonding is the most developed with industrial applications such as silicon-on-insulator structures [4]. The literature on this subject is very extensive but it seems that optical properties of glass/glass bonding for integrated optics components have not been study. We suggest to use this technique for burying optical waveguide with an efficient grating coupler on it.

Manuscript received March 4, 1999; revised December 29, 1999.

S. Pélissier, G. Pandraud, and A. Mure-Ravaud are with the Laboratoire Traitement du Signal et Instrumentation UMR 5516-CNRS-Universite Jean Monnet, 42023 Saint-Etienne Cedex 2, France.

A. V. Tishchenko is with the Institute of General Physics of the Russian Academy of Sciences, Moscow 117942, Russia.

B. Biasse is with LETI, CEA Technologies Avancees, DMITEC-CEN/G, Grenoble Cedex 38054, France.

Publisher Item Identifier S 0733-8724(00)03028-0.

A demonstrator has been done with a waveguide made by ion exchange (K^+/Na^+) which is a common technique for fabrication of graded index planar optical waveguides. However this burying process can be used with other type of waveguides with the same advantages.

The fabrication method presented here allows us to obtain a high radiation coefficient even for a small groove depth and for a grating period compatible with classical photolithographic transfer. The fundamental concepts and formulas used for the design of diffracting grating components are recalled in Section II of the paper. The different steps of the fabrication method are then presented in Section III and a comparison between theoretical design and experimental results is given in Section IV. A conclusion summarizes the advantages and possible applications of this method in other waveguide production technologies.

II. Theoretical Investigations

Many numerical methods exist for the study of diffractive structures and are continuously improved. For the design and the experimental results comparison of our structures, we needed simulation methods. We have then implemented the classical differential method adapted for any waveguide refractive index profile. We also used a new method based on the generalized source method which is explained in [5]. The results given by both methods were verified by comparison on typical structures with rigorous methods based on coupled wave analysis [6], modal technique [7] and improved C-method [8].

A. Methods of Computation

Two types of codes have been used for the simulation of the different studied structures. One has been developed in laboratory TSI and is based on the differential method [9] and on the matrix analysis technique [10]. This code allows us to calculate the performances of any structures and the field intensity profile for incident plane wave but the calculation time is quite long. The second one was developed in the Institute of General Physics of Moscow and is based on a generalized source method [5]. This one is very efficient for calculating radiation coefficients of propagated modes and coupling efficiencies for Gaussian beams with a short calculation time.

Let us consider a dielectric waveguide structure with multiple layers and with a grating as shown in Fig. 1. The cover (index n_c) and the substrate (index n_s) are assumed to be homogeneous with an infinite thickness. A waveguide (index n_w, depth d) and a grating are the intermediate layers. The depth of the grating is p and its period is Λ. For the sake of generalization, the index of the upper part of the grating is n_u and n_b for the bottom. It

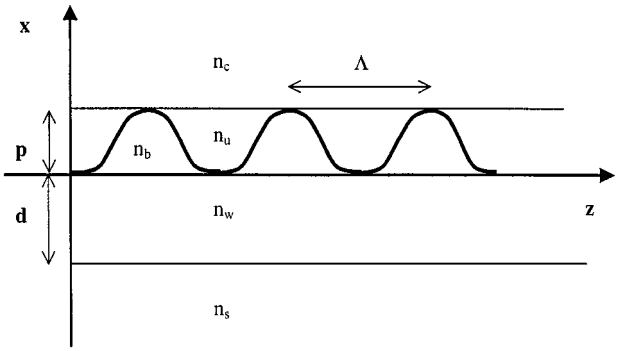

Fig. 1. Notations used for the description of the gratings.

must be noticed that the waveguide may have a constant or a graded index; in this last case, n_w is dependent on x and d is the effective width.

In our case, losses are very low in the waveguide and can be neglected. When the waveguide is corrugated or covered by a grating, the losses become significant and it is possible to define the radiation coefficient. It is assumed in the following that the attenuation of the unperturbed guided mode is very low compared to the attenuation induced by the grating.

For the sake of simplicity, it is assumed that the field is invariant with respect to y and with a time dependence of the form $\exp(-i\omega t)$.

The field in each layer satisfies the scalar Helmoltz equation:

$$(\partial^2/\partial x^2 + \partial^2/\partial z^2)U_j(x,z) + \varepsilon_i \cdot k_0^2 \cdot U_j(x,z) = 0 \quad (1)$$

where U_j is the field component ($U_j = E_{yj}$ for transverse electric (TE) modes and $U_j = H_{yj}$ for transverse magnetic (TM) modes), $k_0 = 2\pi/\lambda_0$ is the free space wave number, ε_j is the dielectric constant and j refers to the layer.

Assuming the field is propagating in the z direction and taking into account the periodic condition due to the grating, the solution of the differential equation (1) can be written in the form [10]

$$\begin{aligned} U_j(x,z) &= \sum_{n=-\infty}^{n=+\infty} f_n^{(j)}(x)\exp(ik_{zn}z) \\ &= \exp(i\beta z)\exp(-\alpha z)\sum_{n=-\infty}^{n=+\infty} f_n^{(j)}(x)\exp(inKz) \end{aligned} \quad (2)$$

where $k_{zn} = \beta + nK + i\alpha$, with $K = 2\pi/\Lambda$ the grating wave number and n the space harmonic number. The real part of k_{zn} is the phase constant of the nth space harmonic and the imaginary part α of k_{zn} is the radiation coefficient due to the leakage of the guided wave energy into the substrate and the superstrate regions.

In the uniform layers, the two-dimensional (2-D) Helmotz equation can be transformed into a one-dimensional (1-D) differential equation:

$$d^2 f_n^{(j)}(x)/dx^2 + \left(k_{xn}^{(j)}\right)^2 f_n^{(j)}(x) = 0 \quad j = c, w \text{ or } s \quad (3)$$

with

$$\left(k_{xn}^{(j)}\right)^2 = \varepsilon_j \cdot k_0^2 - k_{zn}^2.$$

The general solution of this equation is the sum of a copropagative and a contrapropagative plane waves:

$$f_n^{(j)}(x) = a_n^{(j)}\exp\left[ik_{xn}^{(j)}x\right] + b_n^{(j)}\exp\left[-ik_{xn}^{(j)}x\right]. \quad (4)$$

To find the field scattered by the grating [11], an electromagnetic plane wave of unit amplitude is assumed to be incident onto the first or the last interface depending whether the excitation comes from cover ($a_n^{(c)} = 1$ and $a_n^{(s)} = 0$) or the substrate ($a_n^{(c)} = 0$ and $a_n^{(s)} = 1$). Alternatively, to obtain the dispersion relation as well as the harmonic components of guided modes along the grating, we assume no incident wave ($a_n^{(c)} = 0$ and $a_n^{(s)} = 0$).

In the grating region, the periodic permittivity is written in terms of Fourier series:

$$\varepsilon(x,z) = \sum_n \varepsilon_n(x)\exp(2i\pi nz/\Lambda). \quad (5)$$

A similar expression is derived for $\varepsilon(x,z)^{-1}$.

This system can be written as two systems of first-order linear ordinary differential equations and solved by the Runge–Kutta method. The dispersion relation is provided by matching the boundary conditions at both grating layer interfaces and gives the complex propagation constant k_{z0}. The amplitudes of the field in each layer can subsequently be evaluated.

The second method used is an application of the generalized source method [5] to the problem of diffraction of a plane wave on a periodically corrugated interface between two media. In this case, we take $n_c = n_u$ and $n_b = n_w$. The permitivity of the grating layer (Fig. 1) is

$$\varepsilon(x,z) = \varepsilon_w + (\varepsilon_c - \varepsilon_w)\theta[x - \sigma(z)], \quad (6)$$

where $\sigma(z)$ is a periodic function defining the groove shape and $\theta(x)$ is a step function:

$$\theta(x) = \begin{cases} 0, & x < 0 \\ 1, & x > 0. \end{cases} \quad (7)$$

It is considered as a perturbation of the planar waveguide interface located at $x = x_0$

$$\varepsilon = \varepsilon_w + (\varepsilon_c - \varepsilon_w)\theta(x - x_0) \quad (8)$$

by the amendment

$$\delta\varepsilon = (\varepsilon_c - \varepsilon_w)\{\theta[x - \sigma(z)] - \theta(x - x_0)\}. \quad (9)$$

The solution of the unperturbed problem is the sum of incident, reflected and transmitted wave fields

$$\begin{aligned} E_0 &= \theta(x_0 - x)E_I\exp\left(ik_w^0(x - x_0) + ik_z^0 z\right) \\ &\quad + \theta(x_0 - x)E_{0R}\exp\left(-ik_z^0(x - x_0) + ik_z^0 z\right) \\ &\quad + \theta(x - x_0)E_{0T}\exp\left(ik_c^0(x - x_0) + ik_z^0 z\right) \\ &= E_0(x - x_0)\exp\left(ik_z^0 z\right) \end{aligned} \quad (10)$$

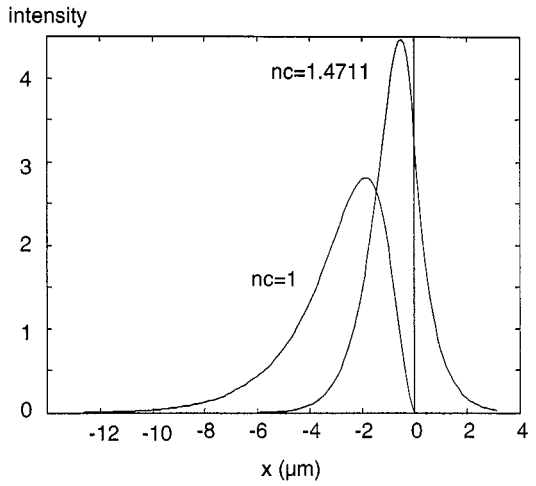

Fig. 2. Theoretical relative intensity of fundamental TE mode for a covered waveguide ($n_c = 1.4711$) and an uncovered one ($n_c = 1$).

where (11) and (12) are shown at the bottom of the next page and the field components of the reflected $\mathbf{E}_{0R}$ and transmitted $\mathbf{E}_{0T}$ waves are taken in accordance with Fresnel formulas.

For the numerical treatment, we divide the thickness of the corrugated region into M layers. In each layer using the z-periodicity of $\delta\varepsilon$ we represent it in a form of a Fourier sum

$$\delta\varepsilon_j = \sum_{q=-\infty}^{\infty} \delta\varepsilon_q(x_j)\exp(iqKz)] \tag{13}$$

where x_j is the ordinate of the center of each layer, and

$$\delta\varepsilon_j^q = \delta\varepsilon^q(x_j) = \frac{K}{2\pi}\int_{-\frac{\pi}{K}}^{\frac{\pi}{K}} (\varepsilon_c - \varepsilon_w) \times \{\theta[x_j - \sigma(z)] - \theta(x_j - x_0)\}\exp(-iqKz)\,dz \tag{14}$$

We define the electromagnetic sources $\mathbf{J}_n$ as the product of the successive solutions $\mathbf{E}_{n-1}$ by the perturbation $\delta\varepsilon$

$$\mathbf{J}_n = -i\omega\delta\varepsilon\mathbf{E}_{n-1}. \tag{15}$$

Taking into account only the restricted number of diffraction orders $-Q \le q \le Q$, the sources can be found in the form of the harmonic sum:

$$\mathbf{J}_{nj}^q = \mathbf{J}_n^q(x_j) = \sum_{q'=-\infty}^{\infty} -\frac{i\omega\delta\varepsilon_j^{q-q'}}{2} \times \theta(x_j - x_0 + h/2)\theta(x_0 - x_j + h/2)\mathbf{E}_{n-1j}^{q'}. \tag{16}$$

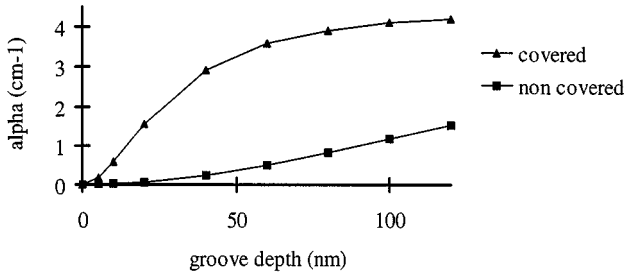

Fig. 3. Theoretical radiation coefficient for covered and uncovered corrugated waveguides.

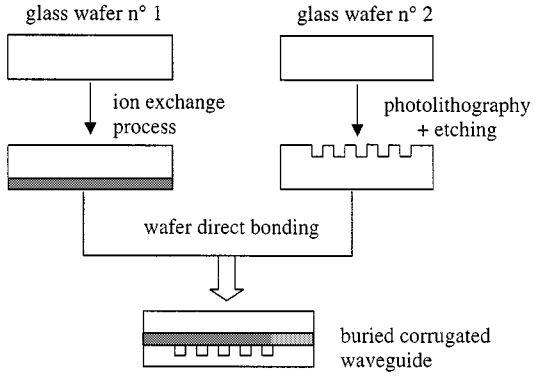

Fig. 4. Process used to obtain buried corrugated waveguide.

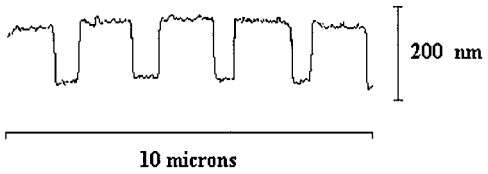

Fig. 5. AFM cross section of the grating used in our demonstrator.

The sources generate the field $\mathbf{E}_n$:

$$E_{nj}^{q\alpha} = -i\omega\sum_{j'=1}^{M}\sum_{\beta=x,y,z}\Gamma_{j-j'}^{q\alpha\beta}\sum_{q'=-Q}^{Q}\delta\varepsilon_{j'}^{q-q'}E_{n-1j'}^{q'\beta}. \tag{17}$$

The final solution is the sum $\sum_{n=0}^{\infty}\mathbf{E}_n$ and can be found by reverting the matrix

$$K_{jj'}^{\alpha\beta qq'} = I_{jj'}^{\alpha\beta qq'} + i\omega\Gamma_{j-j'}^{q\alpha\beta}\delta\varepsilon_{j'}^{q-q'} \tag{18}$$

as the product

$$E_j^{q\alpha} = \sum_{j'=1}^{M}\sum_{\beta=x,y,z}\sum_{q'=-Q}^{Q}[K^{-1}]_{jj'}^{\alpha\beta qq'}E_{j'}^{q'\beta}. \tag{19}$$

$\Gamma_{j-j'}^{\alpha\beta qq'}$ is kernel tensor which components are defined in [5].

$$E_0(x) = \theta(-x)E_I\exp\left(ik_w^0x\right) + \theta(-x)E_{0R}\exp\left(-ik_w^0x\right) + \theta(x)E_{0T}\exp\left(ik_c^0x\right) \tag{11}$$

$$k_j^0 = \begin{cases}\sqrt{\omega^2\mu_0\varepsilon_j - (k_z^0)^2}, & \omega^2\mu_0\varepsilon_j - \left(k_z^0\right)^2 \ge 0;\\ i\sqrt{(k_z^0)^2 - \omega^2\mu_0\varepsilon_j}, & \omega^2\mu_0\varepsilon_j - \left(k_z^0\right)^2 < 0,\end{cases} \quad j = c, w \tag{12}$$

TABLE I

Incident beam I_0	Diffracted order 0 D_0	Diffracted order 1 D_1	Diffracted order 2 D_2
248 mW	195 mW	3.68 mW	1.46 mW

B. Results of Computation

Let us consider a planar waveguide made by ion diffusion in a substrate with surface index n_s. If Δn is the index difference between the surface and the bulk and x is the distance from the surface, the index profile $n_w(x)$ is described by an exponential variation

$$\begin{aligned} n_w(x) &= n_c, && \text{if } x > 0 \\ n_w(x) &= n_s + \Delta n \cdot \exp(-x/d), && \text{if } x \leq 0 \end{aligned} \tag{20}$$

where d is the effective depth.

The following simulations are performed with $n_s = 1.4711$, $\Delta n = 0.008$. The grating has a rectangular profile with $\Lambda = 2$ μm and $d = 1$ μm. These values are justified in Section IV.

Let us see the field repartition in case of TE mode when the waveguide is either at the surface $(n_c = 1)$ or deeply buried $(n_c = n_s)$. It can be seen (Fig. 2) that the field is much more important at the interface in the case of the buried waveguide, furthermore it is also almost symmetric. Consequently, if a grating is fabricated at the interface, with the same index difference (i.e. with air in the groove), it will be more efficient when buried since it is located in an area where a higher intensity field exists.

We have calculated the radiation coefficient in the two following cases when the groove depth p is varied from 0 to 120 nm. In the first case, the cover is air $(n_c = 1)$ and the grating is etched in the waveguide $(n_u = 1; n_b = n_w)$. In the second case, the cover is glass $(n_c = 1.4711)$ and the grating is etched in the cover $(n_u = n_c; n_b = 1)$. The radiation coefficient α is plotted versus the groove depth in Fig. 3. It can be seen that the value of α is ten times greater in the second case than in the first one for small values of p. For p greater than 50 nm, a saturation effect is beginning. The maximum value of α (4.2 cm^{-1}) is sufficient to produce 35% power coupling efficiency in the waveguide for a 2 mm diameter gaussian beam and a 9-mm grating length. These results have been obtained by both methods of computation.

III. Fabrication of the Device

In this section we are going to present the various technologies used to make the waveguide on a first glass wafer, the grating on a second wafer, and finally to bond the two wafers together. The principle of fabrication is summarized in Fig. 4. The material used for the device must be compatible with both the ion exchange process and the bonding technology. For these reasons we have chosen Pyrex 7740 from Corning. This glass is suitable for K^+/Na^+ ion exchange [12] and, as it could be provided in the form of 4″ wafers with a high surface quality, it can be bonded by a low temperature process [13].

The planar waveguide is made on the surface of wafer no. 1 by immersing the wafer in a fused KNO_3 salt at 385°C. The

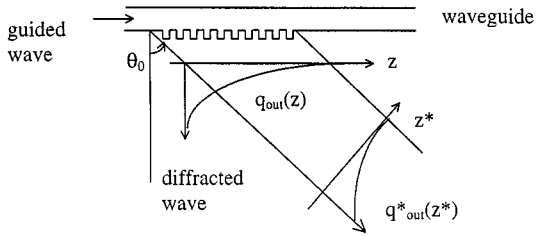

Fig. 6. Outcoupling of light by a grating.

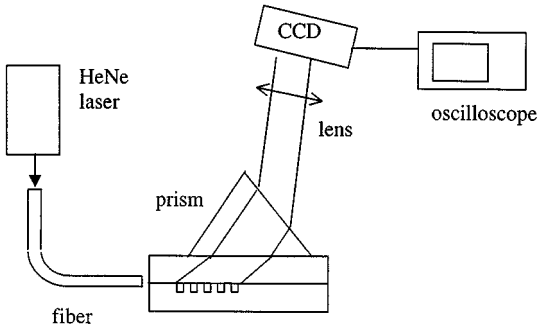

Fig. 7. Experimental setup for the measurement of the intensity profile of the radiated wave.

index profile is given by (20). For Pyrex 7740, n_s is equal to 1.4711; Δn and d are obtained experimentally [14]: Δn is found to be 0.008 and is independent of the time of diffusion, effective depth d is linked to the time of diffusion t and to the diffusion coefficient D by the relation $d = (Dt)^{0.5}$ with $D = 3.59\ 10^{-4}$ μm^2/s. For a time equal to 46 min, d equals 1 μm and it can be shown that this surface waveguide is monomode even when covered by the second wafer [15].

The grating is fabricated on the surface of wafer no. 2 by reactive ion beam etching (RIBE). The first step is to deposit a 1-μm-thick photoresist layer by spin coating. The second step is the photoinscription of the grating in the resist through an amplitude mask. We have used a 2-μm period grating which can be made by classical UV irradiation. After development of the resist, the wafer is ready to be etched. This step has be done by the Institut für Oberflächer Modifizierung (IOM) at Liepzig. An AFM characterization (Fig. 5) shows that the grating has a good rectangular profile but not quite symmetrical. The width of the etched part is smaller than the half period of the grating. This is due to the asymmetry of the photoinduced grating in the resist and could be modify by an optimization of the irradiation process.

The technology used to associate the two previous wafers is a wafer direct bonding (WDB) process developed by LETI-CENG [16]. A brief description of this process is as follows:

TABLE II

	D_0*	D_1*	D_2*	α (cm^{-1})
Experimental values	0.950	0.018	0.007	6
Theoretical values with initial parameters Λ = 2μm p = 127 nm b = 0.31 e = 1 μm Δn = 0,008	0.942	0.021	0.008	8.3
Theoretical values with optimized grating parameters Λ = 2μm p = 120 nm b = 0.3 e = 1 μm Δn = 0.008	0.950	0.018	0.007	8.4
Theoretical values with both optimized parameters Λ = 2μm p = 120 nm b = 0,3 e = 1 μm Δn = 0.0066	0.950	0.018	0.007	6

- hydrophilization of the surfaces;
- rinsing and spin drying;
- simple contact of the two wafers to set off the bonding;
- thermal annealing (350 °C) to stabilize the bonding.

The main advantage of this WDB process is that it requires a temperature (350°C) which is lower than the ion exchange temperature (385°C). The bonding process allows us to bury the grating and the waveguide in order to obtain an original structure of buried corrugated waveguide which could not be made by another technology.

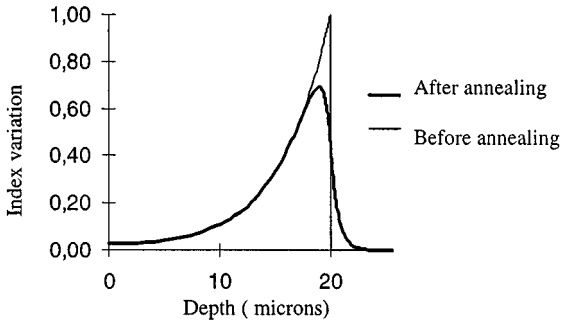

Fig. 8. Modification of the index profile by an annealing.

IV. Characterization of the Device

The characterization of the device has been done by two optical methods.

We measured first the intensities transmitted in the different diffracted orders 0, 1 and 2 in TE polarization with a normal incidence. The results are shown in Table I.

The second measurement was to use the grating as an output coupler for the waveguide and to measure α. It is well known that the amplitude $q_{\text{out}}(z)$ of the output wave radiated by a grating in the θ_0 direction (Fig. 6) can be written in the form: $q_{\text{out}}(z) = A\exp(-\alpha z)$. The setup no. 2 (Fig. 7) enables us to calculate the value of α by measuring the intensity profile $q^*_{\text{out}}(z^*)$. The value of α is found to be $\alpha = 6\ \text{cm}^{-1}$.

These experimental values can be compared with the theoretical results. The geometry used for the computation is similar to Fig. 1, but with rectangular groove profile. The value of Λ, p and b (aspect ratio) can be obtained from the AFM measurements (Fig. 5): $\Lambda = 2\ \mu$m, $p = 127$ nm, $b = 0.31$. The values of d and Δn are given by the characteristics of the ion exchange process: $d = 1\ \mu$m and $\Delta n = 0.008$. The results are shown in Table II. Because of the reflection at the interface air/glass and other additional scattering losses, it is better to compare the ratio of the diffracted intensities, $D_i^* = D_i/(D_0+2D_1+2D_2)$, rather than the values of diffracted intensities D_i/I_0 (where I_0 is the intensity of incident beam, D_i is the intensity of the ith diffracted order). The above initial values of the input parameters $(\Lambda, p, b, d, \Delta n)$ give a reasonably good agreement between theory and experiment since the difference is better than 15% except for α (38%). This could be explained by the lack of accuracy on the values of some parameters. The value of Λ is imposed by the photomask (the process can hardly modify it) and its AFM measurement gives a highly accurate value because it is independent of the shape of the AFM probe. On the contrary the values of p and b are very dependent on the etching process and on the shape of the AFM probe. Then, we can reasonably try to optimize only these two parameters (p and b) in order to obtain a better agreement for the values of D_i^* (Table II). The agreement is still not good for the α value. The waveguide parameters (d and Δn) depend on the ion exchange process. A previous study [17] has shown that during the annealing step of WDB the index profile could be modified as illustrated in Fig. 8. This implies that the value of Δn used in the computation can be different from the initial value. Simulations show that changes in the value of Δn make no modification in the values of D_i^*; only the value of α is modified. This enables to optimize firstly the "grating parameters" (p and b) in order to obtain a good agreement for the values of D_i^* and then to optimize the "waveguide parameter" (Δn) to adjust the value of α.

These results show a very good agreement between theory and experiment with a small change in the initial parameters: the optimized geometry is very close to the values obtained by AFM (5%), the optimized value of Δn is also in the range of expected value.

V. Conclusion

We have shown the interest and the feasibility of buried corrugated waveguide by using a wafer direct bonding technology. Our demonstrator has an higher radiation coefficient than a surface corrugated waveguide. This enable us to design more efficient and compact input or output coupler.

The present low temperature process could be used with other materials than glass and other waveguides than ion exchanged. All the process could be used with the microelectronics technologies. Furthermore, it is the only possibility to fabricate some specific buried device (as for example the buried grating with air in its grooves presented here). Other devices like add-drop filters for example, could be designed with the same original process [14].

References

[1] T. Suhara and H. Nishihara, "Integrated optics components and devices using periodic structures," *IEEE J. Quantum Electron.*, vol. QE-22, pp. 845–867, June 1986.

[2] V. A. Sychugov, A. V. Tishchenko, N. M. Lyndin, and O. Parriaux, "Waveguide coupling gratings for high sensitivity biochemical sensors," *Sensors Actuat. B*, vol. 39, no. 1, pp. 360–364, 1997.

[3] U. Gösele, Q.-Y. Tong, A. Schumacher, G. Kraüter, M. Reiche, A. Plössl, P. Kopperschimdt, T.-H. Lee, and W.-J. Kim, "Wafer bonding for microsystems technologies," *Sensors Actuat. A*, vol. 74, pp. 161–168, 1999.

[4] M. Bruel, "A new silicon on insulator material technology," *Electron. Lett.*, vol. 31, pp. 1201–1202, 1995.

[5] A. V. Tishchenko, "Generalized source method: New possibilities for waveguide and grating problems," Opt. Quant. Electron.. Special Issue on Theoretical Waveguide Modeling, to be published.

[6] M. G. Moharam and T. K. Gaylord, "Diffraction analysis of dielectric surface relief gratings," *J. Opt. Soc. Amer.*, vol. 72, pp. 1385–1392, 1982.

[7] L. Li, "Multilayer modal method for diffraction gratings of arbitrary profile, depth and permittivity," *J. Opt. Soc. Amer.*, vol. 10, pp. 2581–2591, 1993.

[8] T. W. Preist, N. P. K. Cotter, and J. R. Sambles, "Periodic multilayer gratings of arbitrary profiles," *J. Opt. Soc. Amer. A*, vol. 12, pp. 1740–1748, 1995.

[9] R. Petit, *Electromagnetic Theory of Gratings*. Berlin, Germany: Springer Verlag, 1980.

[10] N. H. Sun, J. K. Butler, G. A. Evans, L. Pang, and P. Congdon, "Analysis of grating assisted directional couplers using the Floquet-Bloch theory," *J. Lightwave Technol.*, vol. 15, pp. 2301–2315, 1997.

[11] K. C. Chang, V. Shah, and T. Tamir, "Scattering and guiding of waves by dielectric gratings with arbitrary profiles," *J. Opt. Soc. Amer.*, vol. 70, pp. 804–813, 1980.

[12] J. E. Gortych and G. H. Hall, "Fabrication of planar optical waveguides by K^+ ion exchange in BK7 and Pyrex glass," *IEEE J. Quantum Electron.*, vol. QE-22, pp. 892–895, 1986.

[13] F. Pigeon, B. Biasse, and M. Zusy, "Low-temperature Pyrex glass wafer direct bonding," *Electron. Lett.*, vol. 31, pp. 792–793, 1995.

[14] G. Pandraud, "Dispositifs micro-optiques enfouis par adhérence moléculaire," Thesis, Université Jean Monnet, Saint-Etienne, 1998.

[15] M. J. Adams, *An Introduction to Optical Waveguides*. New York: Wiley, 1981, pp. 113–119.

[16] F. Pigeon and B. Biasse *et al.*, "Procédé de réalisation de guides d'ondes," French patent EN 9408343, European patent EN 95401596.2-2205.

[17] F. Pigeon, S. Pelissier, O. Gipouloux, A. M. Ravaud, G. Pandraud, and B. Biasse, Modelization et caractérisation de l'influence du recuit sur la géométrie d'un guide enterré par la technologie d'adhérence moléculaire, in Journées nationales d'optique guidée, Saint-Etienne, 1997.

S. Pélissier, photograph and biography not available at the time of publication.

G. Pandraud, photograph and biography not available at the time of publication.

A. Mure-Ravaud, photograph and biography not available at the time of publication.

A. V. Tishchenko, photograph and biography not available at the time of publication.

B. Biasse, photograph and biography not available at the time of publication.